Energy Dissipation on Flat-Sloped Stepped Spillways: Part 2. Downstream of the Inception Point

S. L. Hunt, K. C. Kadavy

Abstract. *Many aging watershed dams require hazard classifications changes. As a result, these dams may no longer meet state and federal dam safety regulations because of inadequate spillway capacity and flood protection. Rehabilitation options for these embankments are often limited due to encroaching urban development. Roller compacted concrete (RCC) stepped spillways are a popular choice in these situations because the spillway capacity can be increased with little or no additional changes to the embankment dimensions. RCC stepped spillways are also selected because of the cost and time savings in the construction of these structures. Design engineers require more information about the inception point location and the approach velocity and energy dissipation in the spillway chute. These elements are important for properly dimensioning the spillway training walls and stilling basin. Research and more specifically design guidelines for RCC stepped spillways applied to small earthen embankments have been limited. A two-dimensional, physical model was constructed to evaluate the inception point, velocities, air concentrations, and energy dissipation in a 4(H):1(V) slope spillway chute having 38 mm (1.5 in.) high steps. Model unit discharges ranging from 0.11 $m^3 s^{-1} m^{-1}$ (1.2 cfs ft^{-1}) to 0.82 $m^3 s^{-1} m^{-1}$ (8.8 cfs ft^{-1}) were tested. The findings from this research show that a relationship developed by H. Chanson can be used to determine the inception point location on stepped chutes with Froude surface roughness (F_*) ranging from 10 to 100 for slopes as flat as 4(H):1(V). Additionally, air concentrations near the inception point are approximately 0% and rapidly increase to 10% slightly downstream of the inception point. These air concentrations continue to increase gradually to a constant as the flow descends the chute. The study results show that energy losses increase from 30% when a normalized length (L/L_i and L/L_{i*}) equals 1 to 73% when L/L_i and L/L_{i*} equals 3.5. A first attempt at providing an energy loss relationship at any point downstream of the inception point is provided. This research will assist engineers with the design of stepped spillways applied on relatively flat embankment dams.*

Keywords. *Air entrainment, Dam rehabilitation, Energy dissipation, Flood control, Inception point, Physical modeling, Roller compacted concrete (RCC), Stepped spillways, Stilling basin.*

Roller compacted concrete (RCC) stepped spillways are not a new technology. According to Chanson (2002), stepped chutes have been around for centuries. In recent years, their popularity has increased for the rehabilitation of aging flood control dams. This technology is expected to be applied to thousands of small flood control dams. RCC stepped spillways provide a means for increasing the capacity of existing flood control structures. Modifications to the dimensions of the existing dam are often not required in conjunction with stepped spillways, thereby making them more desirable over other rehabilitation designs. Additionally, RCC has cost and construction time advantages when compared to conventional concrete. In most dam rehabilitations, stepped spillways are placed over the existing earthen embankment; thus, the slope of the spillway is the same as the downstream slope of the dam. Typical face slopes of earthen embankments are 2(H):1(V) or flatter.

Stepped spillway research for these flatter applications is limited, and design guidelines are scarce. Without model studies, the safety and integrity of a flat stepped spillway may be questioned, or the design may be overly conservative, leading to a more expensive project. The USDA Agricultural Research Service (ARS) Hydraulic Engineering Research Unit (HERU) is conducting research on stepped spillways constructed on existing embankment dams. Air entrainment and energy dissipation in flatter (2(H):1(V) or flatter) stepped spillways may affect the design of the spillway training walls and the stilling basin differently than steeper (2(H):1(V) or steeper) stepped spillways. Therefore, the USDA-ARS HERU is currently conducting research to evaluate the effects that a 4(H):1(V) stepped spillway chute has on the inception point location, air concentrations, velocities, and the energy dissipation for a specified range of skimming flows. This article reports on research results on spillway performance downstream of the inception point. This research will assist engineers in the design of these structures.

Submitted for review in April 2009 as manuscript number SW 7985; approved for publication by the Soil & Water Division of ASABE in December 2009.

The authors are **Sherry L. Hunt, ASABE Member Engineer,** Research Hydraulic Engineer, and **Kem C. Kadavy, ASABE Member Engineer,** Agricultural Engineer, USDA-ARS Hydraulic Engineering Research Stillwater, Oklahoma. **Corresponding author:** Sherry L. Hunt, USDA-ARS Hydraulic Engineering Research Unit, 1301 N. Western St., Stillwater, OK 74075; phone: 405-624-4135, ext. 222; fax: 405-624-4136; e-mail: Sherry.Hunt@ars.usda.gov.

Background

Design engineers of stepped spillways have expressed interest in the affects of air entrainment and energy dissipation

on spillway and stilling basin design. Design guidelines are limited for stepped spillways, especially on the flatter stepped spillways associated with small embankment dams. Peyras et al. (1992), Rice and Kadavy (1996), Yasuda and Ohtsu (1999), Chanson (2002), Chanson and Toombes (2002), Boes and Hager (2003a, 2003b), Takahasi et al. (2006), Hunt et al. (2006), Hunt and Kadavy (2007, 2008), and Felder and Chanson (2008), among others, have researched flat (2(H):1(V) or flatter) stepped spillways. Each has contributed to the understanding of these structures in some fashion. For instance, Peyras et al. (1992) discussed the flood flows that gabion-style stepped spillways can withstand, and the cost savings for using this material in spillway design. Rice and Kadavy (1996) reported on a specific model study of a stepped spillway on a 2.5(H):1(V) slope and indicated that energy dissipation was significantly more in a stepped spillway when compared to a smooth spillway with the same chute slope. Chanson (2002) compiled extensive literature regarding stepped spillways concerning scaling effects that occur in stepped spillway modeling, differences in nappe and skimming flow regimes, and development of relationships for inception point location and energy dissipation. Chanson and Toombes (2002) reported energy dissipation rates where the ratio of head loss to total head was approximately 0.8 for slopes of 11(H):1(V) or flatter, and reported that the air concentration distributions were similarly shaped for smooth and stepped spillways under skimming flow regimes.

Modeling air-entrained flows can be difficult due to scale effects. Scale effect describes slight distortions that are introduced in modeling when viscous forces and surface tension in highly air-entrained flows are ignored. Boes (2000), Chanson (1994a), Boes and Hager (2003a, 2003b), and Takahashi et al. (2006) have provided guidance to other researchers on modeling techniques for reducing scale effects associated with air-entrained flows. Generally, a scale of 10:1 or larger is an accepted scale for modeling stepped spillways (Chanson, 2002). Boes and Hager (2003a) recommend a Reynolds number of 10^5 and a minimum Weber number of 100, respectively, to minimize scale effects.

The inception point (fig. 1) is valuable in the design of stepped spillways because it indicates the location where significant flow bulking first occurs. The inception point is the location where the turbulent boundary layer reaches the free surface. Flow bulking is the increased flow depth created by the mixture of air and water. As shown in figure 1, this flow bulking occurs downstream of the inception point. If the inception point occurs upstream of the expected design tailwater and stilling basin, then the engineer should consider increasing the training wall height to account for this increase flow depth. Stepped spillways applied to existing embankments typically have a relatively short spillway chute and high design flow. Consequently, the inception point often occurs downstream of the expected tailwater or in the stilling basin. In these cases, flow bulking has little impact on training wall design; however, the inception point location should be examined for each situation. Chanson (1994a) developed a relationship to determine the inception point location for primarily steep (2(H):1(V) or steeper) stepped spillways. Hunt and Kadavy (2007, 2008) determined that Chanson's relationship can be applied to stepped spillways with chutes as flat as 4(H):1(V) for a Froude surface roughness (F_*) ranging from 10 to 100 (Hunt and Kadavy, 2009).

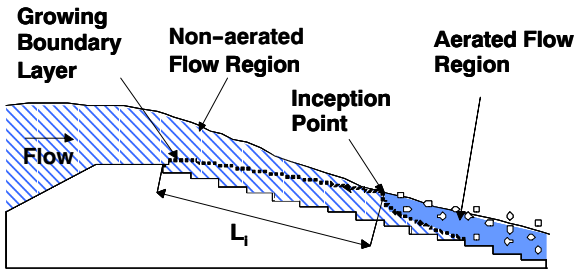

Figure 1. Schematic of the inception point in relation to the stepped spillway.

Another key component in the design of the stepped spillway is the energy dissipation that occurs in the spillway chute. Extensive research has been conducted on energy dissipation, including work by Christodoulou (1993), Boes (1999), Chanson, (2002), Chanson and Toombes (2002), Chatila and Jurdi (2004), and Barani et al. (2005). The majority of this research was conducted on steep (2(H):1(V) or steeper) stepped spillways. Christodoulou (1993) discovered that the most important parameters governing energy dissipation are the ratio of the critical depth to the step height and the number of steps. Boes (1999) and Chatila and Jurdi (2004) indicate that energy dissipation is significantly larger in stepped spillways than conventional smooth spillways and that energy dissipation increases with increasing step height for a given spillway. Chanson (2002) suggests that greater energy dissipation occurs in stepped spillways under nappe flow conditions (i.e., water flows down a stepped spillway in a succession of free fall jets), which most likely occurs in stepped spillways with large step heights on relatively flat slopes. However, the maximum design flow in these particular spillways is rarely nappe flow.

The objective of this article is to provide velocity as obtained by multiple measurement techniques, air concentration, and energy loss data downstream of the inception point for a range of flows. This generalized model study was conducted on a 4(H):1(V) slope stepped spillway. Specifically, this article provides a generalized relationship for determining energy losses at any point downstream of the inception point for a 4(H):1(V) stepped spillway. For small embankment dams, the design flow is expected to be large, and the stepped spillway chute is expected to be relatively short compared to large gravity dams. In these instances, fully developed air-entrained flow may not be achieved within the spillway chute. In limited cases, air entrainment may fully develop at the free surface; consequently, flow bulking downstream of the inception point would be expected. The air-entrained data are the primary focus of this article. Flow bulking directly impacts the design of the training walls for the spillway chute and the stilling basin. Additionally, energy dissipation and velocities are important to properly size the stilling basin. Therefore, this research is useful in the design of stepped spillways and their stilling basins applied to small embankment dams.

Experimental Setup

A two-dimensional model of a stepped spillway was constructed for a generalized study to evaluate the inception point, air concentrations, velocities, and energy losses asso–

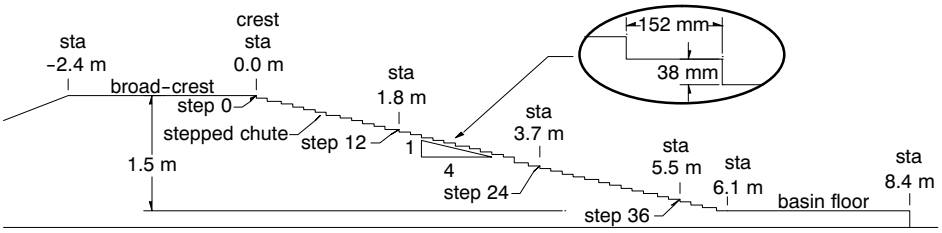

Figure 2. Schematic of stations on a stepped spillway model.

ciated with flood flows. The model was constructed across the full width of a 1.8 m (6 ft) flume. The flume walls are 2.4 m (8 ft) tall, and the spillway model has a vertical drop of 1.5 m (5 ft). The model was constructed with a broad-crested weir, and the chute slope is 4(H):1(V). Step heights of 38 mm (1.5 in.) were placed in the model. The downstream edge of the weir corresponds to station 0.0 m (0.0 ft) and step 0. The downstream toe of the spillway is at station 6.1 m (20 ft) at step 40. Figure 2 illustrates the two-dimensional model.

To minimize scale effects associated with the collection of data in air-entrained flow environments, the criterion suggested by Boes and Hager (2003a) was followed, and a scale of 10:1 or larger is recommended. Reynolds and Weber numbers for this generalized model study were reported by Hunt and Kadavy (2008, 2010). Water surface elevations and velocity measurements were collected. A moveable carriage set atop rails on the flume walls allowed manual point gauge readings of the centerline water and bed surface elevations. The carriage was also used to collect centerline velocity measurements at the crest. A second set of rails was attached to the flume walls and set parallel to the sloping chute. These rails were used for velocity measurements along the centerline of the chute. Figure 3a illustrates the use of the carriage for recording flow measurements, and figure 3b illustrates velocity measurement collection normal to the chute slope.

Unit discharges of 0.11, 0.20, 0.28, 0.42, 0.62, 0.82 $m^3 s^{-1} m^{-1}$ (1.2, 2.2 3.0, 4.5, 6.7, 8.8 cfs ft^{-1}) were tested. Cross-sectional velocity profiles were collected with an acoustic Doppler velocimeter (ADV) on the broad-crested weir to develop a calibration curve of the flow versus upstream head. Velocity profiles and flow depths were collected along the centerline of the spillway using three separate measuring devices: (1) an ADV, (2) a pitot tube (PT) coupled with a differential pressure transducer, and (3) a two-tip fiber optical (FO) probe and data acquisition system. Each device has a unique range of velocities that could be captured during testing. The ADV was limited by a maximum velocity of 4.6 m s^{-1} (15 ft s^{-1}), and it could not be used in highly turbulent flow. The PT coupled with a pressure transducer has the advantage of collecting higher velocities than the ADV. The PT also provides verification for some of the velocity measurements collected with the ADV. Matos et al. (2002) found that the PT can be used in air-entrained environments when the air concentrations in the flow are less than 70%, thereby giving it another advantage over the ADV. To achieve more accurate velocity measurement in air-entrained flows, the PT was back-flushed before each measurement to remove air bubbles in the tube and the lines to the pressure transducer. The two-tip FO probe was used to measure velocities and void fraction (C) in air-entrained flows. The void fraction data collected by the FO probe was used to determine the equivalent clear water depth that would result without the presence of the entrained air.

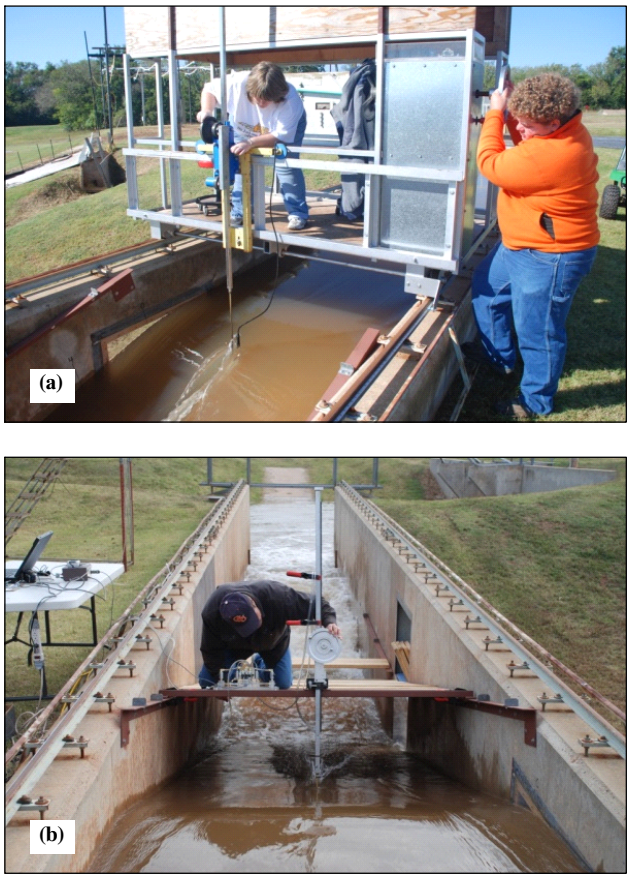

Figure 3. (a) Data collection using a mobile carriage along the top of the test flume walls, and (b) data collection using secondary rails set parallel to the sloping chute.

Velocity profiles were taken normal to the spillway crest surface along the centerline at horizontal stations -2.4, -1.8, -1.2, -0.61, 0.0 m (-8, -6, -4, -2, and 0 ft) (fig. 2) with the ADV. Velocity profiles normal to the spillway chute slope along the centerline were taken at horizontal stations 0.0, 0.61, 1.2, 1.8, 2.4, 3.0, 3.7, 4.3, 4.9, and 5.5 m (0, 2, 4, 6, 8, 10, 12, 14, 16, and 18 ft) (fig. 2) with the ADV when the velocities were within its limits, with the PT for all stations on the chute, and with the FO probe when air entrainment was present. These horizontal stations correspond to the downstream edge of the step. Two velocity profiles were taken with the PT and the FO probe along the stilling basin floor. These measurements were taken normal to the floor at horizontal stations 6.6 and 8.1 m (22 and 27 ft), respectively.

PT velocity measurements were collected starting near the step edge surface and incrementally moved up the depth profile. The ending measurement was the highest point in the depth profile at which the flow still appeared as a coherent

stream of water. This ending point normally corresponded to a point void fraction of approximately 0.5. For the velocity profile analysis, velocities above this point were assumed to be equal to the velocity at the last measured depth.

FO velocity and void fraction measurements were collected starting at the upper surface of the depth profile where the void fraction was approximately 0.95 and incrementally moved down the depth profile to the step edge surface or to the depth at which the void fraction was so small that measurements could not be collected. The FO void fraction data was used for the FO and PT velocity profile analysis.

Results and Discussion

An important element in stepped spillway chute training wall design is whether to account for flow bulking. As the turbulent boundary layer nears the free surface, the flow appearance changes. The inception point is detected when the boundary layer reaches the free surface. Figure 1 illustrates the inception point development. The growing boundary layer is generated by the friction of the stepped surface. In the case of the stepped spillway, the growing boundary layer typically begins at the spillway crest. For a broad-crested weir spillway, the growing boundary layer, as Hunt and Kadavy (2010) define it, begins at the downstream edge of the weir. Although a small amount of boundary layer development may occur upstream of this point on the smooth crest surface, it is considered insignificant compared to the development that occurs downstream of this point on the stepped chute surface. Chanson (1994a, 2002) characterizes the inception point as the location where the turbulent boundary layer reaches the free surface. Upstream of the inception point, the flow is described as non-aerated, as shown in figure 1. Downstream of the inception point, an aerated flow region is established, and this region becomes more fully developed as the flow moves further downstream.

As previously reported by Hunt and Kadavy (2008), flow was observed to change from a glassy, smooth appearance to a slight undulating appearance to a white water or frothy appearance. The slight undulating appearance was noted during testing as the turbulent boundary layer approaching the free surface. When the flow at the surface appeared frothy across the full width of the flume, the turbulent boundary layer was thought to have reached the free surface, and that location was recorded as the inception point. Hunt and Kadavy (2007, 2008) found that an inception point relationship developed by Chanson (1994b, 2002) can be used to determined the inception point location in stepped spillway slopes as flat as 4(H):1(V) even though the original relationship was developed from steep (2(H):1(V) or steeper) stepped spillways. This relationship was verified for Froude surface roughness (F_*) ranging from 10 to 100 (Hunt and Kadavy, 2009). Chanson's relationship, as indicated by equation 1, is based on the spillway chute slope, unit discharge, gravitation acceleration, and step height (0.038 m in this study):

$$L_{i*} = 9.719(\sin\theta)^{0.0796}(F_*)^{0.713}h(\cos\theta) \quad (1)$$

where

L_{i*} = distance from the start of growth of boundary layer to the inception point of air entrainment
θ = channel slope
F_* = Froude number defined in terms of the roughness height ($F_* = q/[g(\sin\theta)\{h(\cos\theta)\}^3]^{0.5}$)
h = step height
q = unit discharge
g = gravitational constant.

Hunt and Kadavy (2010) identify the downstream edge of the broad-crested weir as the origin point for length to the inception point (fig. 1). Table 1 shows F_* for all tested flows and how closely the inception point (L_{i*}) as calculated using equation 1 compares to the inception point (L_i) observed by Hunt and Kadavy (2008). These results are valid when F_* ranges from 10 to approximately 100 (Hunt and Kadavy, 2009). Some of the differences between the observed and predicted inception points are likely due to the subjectivity of the visual observations. In particular, the observed and predicted inception points for the unit discharge of 0.62 $m^3 s^{-1} m^{-1}$ (6.7 cfs ft^{-1}) showed a 14% difference. The inception point for this discharge was near the break in slope from the spillway chute to the stilling basin, so this slope change may have influenced the observed inception point location. The predicted inception point location for unit discharge of 0.11 $m^3 s^{-1} m^{-1}$ (1.2 cfs ft^{-1}) is 21% larger than the observed inception point location, and this difference may be partially attributed to F_* equaling 10, the recommended minimum for the use of equation 1.

The results summarized in table 1 are valuable to design engineers. The inception point location in relation to the stilling basin and the design tailwater provides the necessary information for the design engineer to make an informed decision on whether flow bulking should be accounted for in the design of the stepped spillway training walls.

Additional information valuable to the design engineer is the energy dissipation that occurs in the spillway chute. Stepped spillways dissipate a significant amount of energy when compared to traditional smooth chute spillways. Consequently, the stilling basin size can be reduced for a stepped spillway as compared to a stilling basin for a traditional smooth chute spillway of similar size. To determine the energy loss in the spillway chute, velocity must be determined. Figures 4a through 4e present typical depth-velocity profiles measured with the PT and FO probe and the depth-void fraction (C) measured with the FO probe at stations 3.0 (10 ft), 3.7 (12 ft), 4.3 (14 ft), 4.9 (16 ft), and 5.5 m (18 ft) for a unit discharge of 0.28 $m^3 s^{-1} m^{-1}$ (3.0 cfs ft^{-1}). Figure 4a represents a velocity and void fraction (C) profile just upstream of the inception point at L/L_i = 0.96, while figures 4b through 4e represent profiles downstream of the inception point at L/L_i = 1.2, 1.4, 1.6, and 1.7, respectively. Figures 4a through 4e show similarities in the velocity data from the PT and the FO probe. In figures 4a and 4b, the velocities near the spillway chute bed surface were undetectable by the FO probe because the air concentrations were significantly low or nonexistent. The PT provides a

Table 1. Calculated and observed inception point data for each of the flows.

		Chanson (1994b)		Observed	
q ($m^3 s^{-1} m^{-1}$)	F_*	L_{i*} (m)	Inception Point (step)	L_i (m)	Inception Point (step)
0.82	75	7.0	Basin	7.1	Basin
0.62	57	5.7	36	6.6	Basin
0.42	38	4.3	28	4.6	29
0.28	26	3.2	21	3.5	22
0.20	18	2.6	17	2.7	17
0.11	10	1.7	10	1.4	9

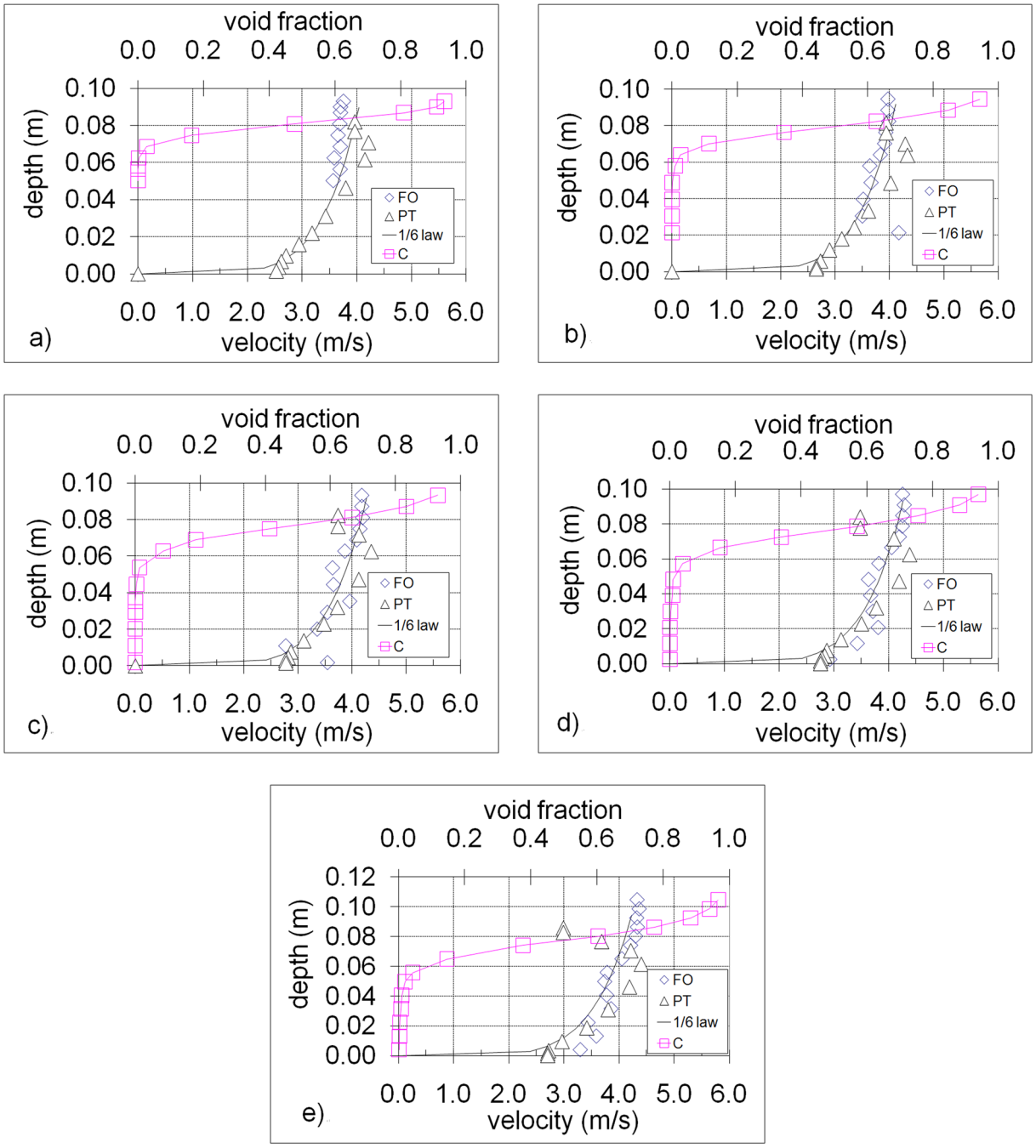

Figure 4. Depth-velocity and depth-void fraction (*C*) for a unit discharge of 0.28 m^3 s^{-1} m^{-1} (3.0 cfs ft^{-1}): (a) station 3.0 m (10 ft), (b) station 3.7 m (12 ft), (c) station 4.3 m (14 ft), (d) station 4.9 m (16 ft), and (e) station 5.5 m (18 ft).

record of the velocities in these lower portions of the profiles, giving it an advantage over the FO probe. In figures 4a through 4c, the velocity profiles measured with the PT and the FO probe yield similar results, indicating that the air concentration likely does not influence the PT results. Separation between the two profiles is noticeable in figures 4d and 4e near the flow surface. The difference in the profile is likely attributed to the more fully developed air in the profile, yet upon further examination, the average velocities for the PT and FO probe data for figure 4d are 3.70 m s^{-1} (12.2 ft s^{-1}) and 3.69 m s^{-1} (12.1 ft s^{-1}), respectively. For figure 4e, the average velocities for the PT and FO data are 3.71 m s^{-1} (12.2 ft s^{-1}) and 3.73 m s^{-1} (12.3 ft s^{-1}), respectively. Based on this observation, the air concentration in the flow appears small enough that it does not affect the average velocity when velocities are measured with the PT. Additional observations were made regarding the velocity profiles. For instance, in previously reported research, Hunt and Kadavy (2008) showed that the velocity profiles transition from uniform at the crest to approaching a one-sixth power law distribution at the inception point for all tested flows. Boes and Hager (1998) and Chanson (2000) also determined that the velocity profiles tended to follow a one-sixth power law distribution. Figures 4a through 4e show that the velocity profiles follow a one-sixth power law distribution at and downstream of the inception point.

Figures 4a through 4e also illustrate depth-void fraction profiles. At each station, the void fraction increases dramatically from 0% at the bed surface to near 95% at the water surface (figs. 4a through 4e). The void fraction data were used to determine the equivalent clear water depth (y_{cw}) for each station. For air-water flows, the y_{cw} as defined by Chanson et al. (2002) is:

$$y_{cw} = \int_0^{y_{90}} (1 - C) * dy \qquad (2)$$

where y_{90} is characteristic depth (m) when the air concentration is 90%, and C is air concentration, which is also known as void fraction. Upstream of the inception point, the measured depth is equal to the clear water depth because there is very little if any air present. Downstream of the inception point, air is visibly present. Therefore, the y_{cw} downstream of the inception point is the equivalent depth of flow with no air present. Figure 5 illustrates the y_{cw}-velocity profile for station 5.5 m (18 ft). When figure 5 is compared to figure 4e, the y_{cw} is clearly less in figure 5 as compared to the flow depth with air in figure 4e. The clear water depth information is needed to determine the average air concentration in the flow as well as the energy dissipation. As defined by Boes and Hager (2003a), the average air concentration, C_{avg}, is:

$$C_{avg} = 1 - \frac{y_{cw}}{y_{90}} \qquad (3)$$

The average air concentrations for each flow rate and station were plotted against the log of the normalized length down the spillway chute (i.e., length from the downstream crest edge to the location of interest parallel to the spillway chute, L, normalized by the inception point location, L_i). Upstream of the inception point, the air concentration is 0%. By definition, the average air concentration is 0% at the inception point, L/L_i and predicted L/L_{i*}, equal to 1. Slightly downstream of the inception point, the air concentration increases to 10% (fig. 6). The air concentration continues to increase gradually until it reaches a constant value as the flow descends farther downstream of the inception point. Figures 6a and 6b also demonstrate the similarity between the average air concentrations versus the normalized length down the spillway chute using both the observed and predicted inception point locations.

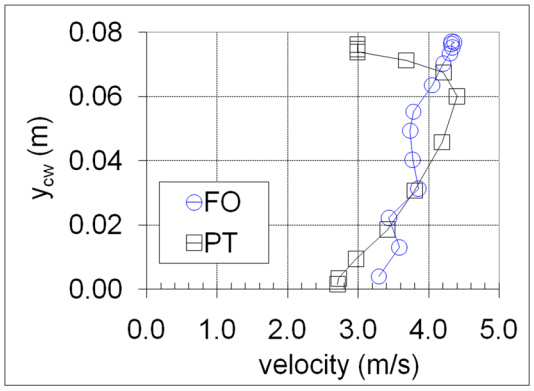

Figure 5. Clear water depth (y_{cw}) velocity profiles at station 5.5 m (18 ft) for a unit discharge of 0.28 m^3 s^{-1} m^{-1} (3.0 cfs ft^{-1}).

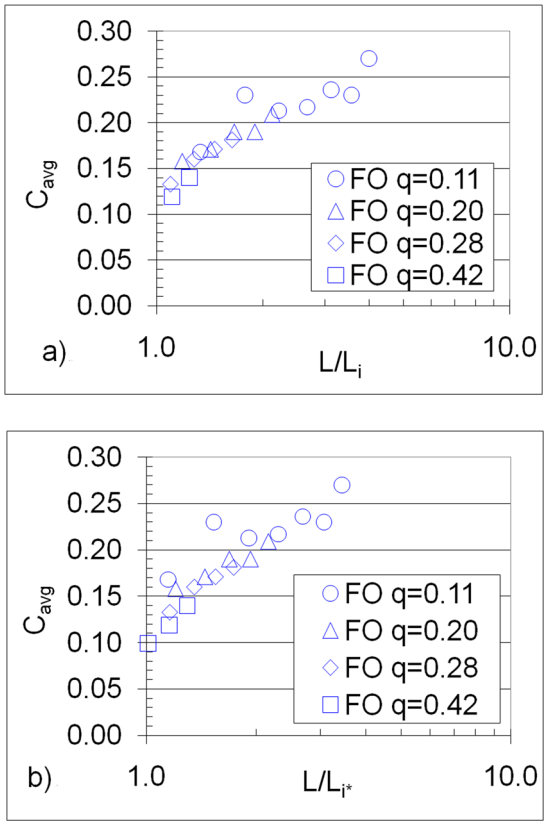

Figure 6. (a) Average air concentration (C_{avg}) versus the normalized length down the spillway chute (L/L_i) based on observed L_i, and (b) average air concentration (C_{avg}) versus the normalized length down the spillway chute (L/L_{i*}) based on calculated L_{i*}.

The average velocity obtained from the velocity profiles was used to determine the energy loss on the spillway chute downstream of the inception point. The average velocity was based on y_{cw}, as illustrated in a single example in figure 5. With the average velocity at each station known, the total energy loss to a given step relative to the step of interest can be determined:

$$\Delta H = H_o - H \qquad (4)$$

where

$$H_o = y_o + \frac{V_o^2}{2g}$$

$$H = y_{cw} \cos\theta + \alpha \frac{V_{cw}^2}{2g}$$

V_{cw} = clear water mean velocity
V_o = approach velocity
y_o = approach depth above datum
y_{cw} = clear water flow depth
θ = chute slope
g = gravitational acceleration
α = energy coefficient.

Figure 7 illustrates the energy loss parameters as they relate to the stepped spillway. The datum line is at the elevation of the step of interest. In many open-channel applications where the channel is of regular cross-section with fairly straight alignment, the energy coefficient (α) is assumed to equal unity because the effect of non-uniform velocity distribution on the computed velocity head and momentum is small (Chow, 1959). To determine the effect that the non-uniform velocity distribution has on the compu-

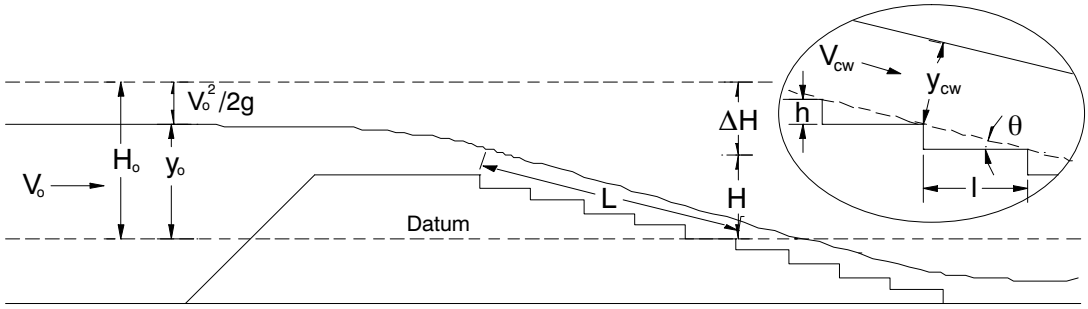

Figure 7. Energy loss parameters as they relate to the stepped spillway.

ted velocity head and momentum, equation 5 was used to determine the energy coefficient:

$$\alpha = \frac{\int v^3 dA}{V_{cw}^3 A} \approx \frac{\sum v^3 \Delta A}{V_{cw}^3 A} \quad (5)$$

where v is the point velocity for an incremental area (ΔA) in the velocity profile, V_{cw} is the mean velocity of the equivalent clear water depth-velocity profile, and A is the total area of the profile. Assuming two-dimensional flow that is uniform across the width, the area (A) could be replaced by y_{cw}. As shown in figure 8, the energy coefficient ranges from 1.01 to 1.07. This energy coefficient range is reasonable when compared to the values of 1.05 to 1.1 reported by Boes (1999) for fully air-entrained flows.

With the energy coefficient data determined, equation 4 was used to determine the energy loss in the stepped spillway. Hunt and Kadavy (2008, 2010) reported that the energy loss follows a linear trend upstream of the inception point. The energy loss relationship upstream of the inception point provided by Hunt and Kadavy (2008, 2010) is:

$$\frac{\Delta H}{H_o} = 0.3 * \frac{L}{L_{i*}} \quad (6)$$

Figure 9 presents the energy loss data downstream of the inception point. Figure 9a illustrates the energy loss verses the normalized length down the spillway chute observed during the test (L/L_i). Figure 9b shows the relationship of the relative energy loss versus the normalized length down the spillway chute using the inception point as calculated by equation 1 (L/L_{i*}). These figures demonstrate the similarity between the relative energy loss versus the normalized length down the spillway chute using both the observed and predicted inception points. When the observed ratio L/L_i and computed L/L_{i*} is equal to 1, then the energy loss is approximately 0.30 for all tested flows. Downstream of the inception point, the energy loss increases to approximately 0.73 for values of L/L_i and L/L_{i*} of 3.5. The data in figure 9a were fit with a power relationship using two constraints: (1) at $L/L_i = 1.0$, $\Delta H/H_o = 0.30$ and (2) at $L/L_i = \infty$, $\Delta H/H_o = 1.0$. The resulting equation (eq. 7) represents the data well and is illustrated in figure 9a. Based on these findings, the relative energy loss at any point downstream of the inception point may be approximated by the following relationship:

$$\frac{\Delta H}{H_o} = 1 - \left(\frac{L}{L_{i*}} + 0.51 \right)^{-0.87} \quad (7)$$

Differences between the fit of equation 7 and the data illustrated in figure 9b are attributed to a breakdown in the predicted inception point relationship provided in equation 1.

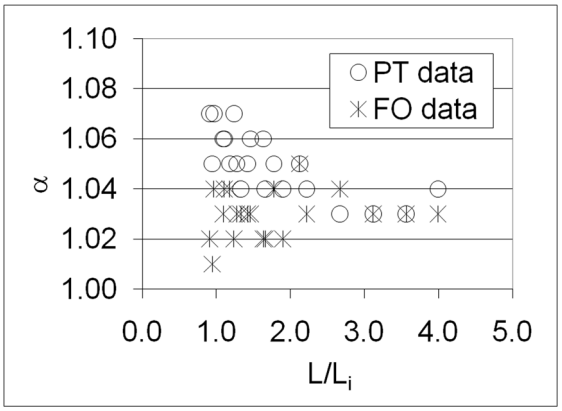

Figure 8. Energy coefficient (α) versus the normalized length (L/L_i) down the spillway chute.

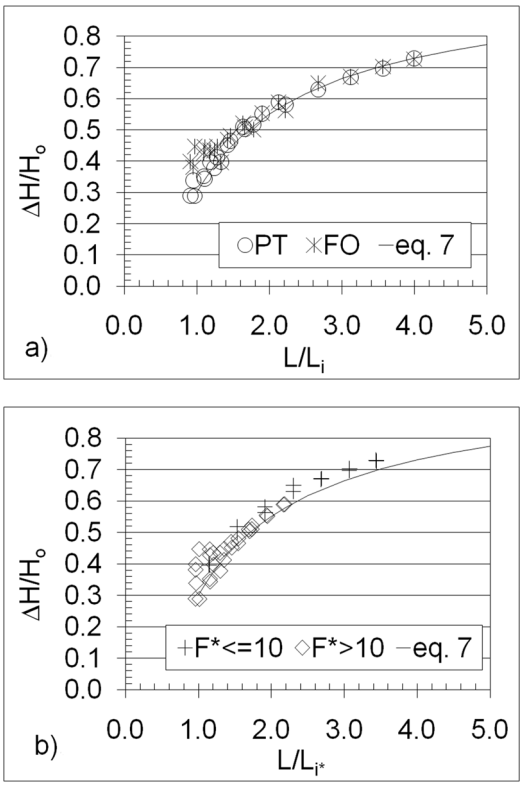

Figure 9. (a). Relative energy loss versus the normalized length down the spillway chute based on observations, and (b) relative energy loss versus the normalized length down the spillway chute based on the predicted inception point location.

For a Froude surface roughness (F_*) greater than 10, equation 7 appears to fit the data well, but when F_* is equal to or less than 10, equation 7 begins to underestimate the energy loss. From this observation, it is concluded that equation 7 should be limited for use with equation 1 for F_* greater than 10. This is a first attempt at providing an energy loss relationship downstream of the inception point. Additional data from other tested step heights is expected to improve this relationship.

CONCLUSIONS

Many small earthen flood control dams are faced with inadequate spillway capacities due to permanent pools filled with sediment and sediment depositing in the flood pools. Additionally, many small flood control dams have experienced changes in hazard classification. Urbanization is the cause of most changes in the hazard classification of these structures. Many engineers are selecting RCC stepped spillways as a rehabilitation design for these structures in order to comply with dam safety regulations.

This model study provides details regarding the design of a stepped spillway on a 4(H):1(V) slope. Based on observations and data collected, a relationship developed by Chanson (1994a) may be used to determine the inception point on stepped spillway chutes as flat as 4(H):1(V) when F_* ranges between 10 and 100. Velocity profiles recorded with a PT and FO probe downstream of the inception point resulted in similar average velocities. Therefore, accurate velocities can be measured using a PT in air-entrained flows. As reported by Hunt and Kadavy (2008), velocity profiles transition from uniform at the crest to a one-sixth power law distribution near the inception point. Velocity profiles continue to follow a one-sixth power law distribution downstream of the inception point. Air concentrations near the inception point are approximately 0% for all flows and rapidly increase to 10% slightly downstream of the inception point. After this point, the air concentrations gradually increase to a constant value as the flow descends the chute. Additionally, a first-generation relationship for determining the energy loss at any point downstream of the inception point was provided. Energy losses increased from 30% for L/L_i and L/L_{i*} equal to 1 to 73% for L/L_i and L/L_{i*} equal to 3.5. Additional data have been collected from this model to compare the effects of different step heights on the inception point, velocities, air concentrations, and energy dissipation; these data are currently under analysis. This research will assist engineers with the design of stepped spillways and their associated stilling basins when applied on relatively flat embankment dams.

REFERENCES

Barani, G. A., M. B. Rahnama, and N. Sohrabipoor. 2005. Investigation of flow energy dissipation over different stepped spillways. *American J. Applied Sci.* 2(6): 1101-1105.

Boes, R. M. 1999. Physical model study on two-phase cascade flow. In *Proc. 28th IAHR Congress*, Session S1. International Association for Hydro-Environment Engineering and Research.

Boes, R. M. 2000. Scale effects in modelling two-phase stepped spillway flow. In *Proc. Intl. Workshop on Hydraulics of Stepped Spillways*, 53-60. H. E. Minor and W. H. Hager, eds. Steenwijk, The Netherlands: A. A. Balkema.

Boes, R. M., and W. H. Hager. 1998. Fiber-optical experimentation in two-phase cascade flow. In *Proc. Intl. RCC Dams Seminar.* K. Hanson, ed. Denver Colorado, Schabel Engineering.

Boes, R. M., and W. H. Hager. 2003a. Two-phase flow characteristics of stepped spillways. *J. Hydraul. Eng. ASCE* 129(9): 661-670.

Boes, R. M., and W. H. Hager. 2003b. Hydraulic design of stepped spillways. *J. Hydraul. Eng. ASCE* 129(9): 671-679.

Chanson, H. 1994a. Hydraulics of skimming flows over stepped channels and spillways. *IAHR J. Hydraul. Res.* 32(3): 445-460.

Chanson, H. 1994b. *Hydraulic Design of Stepped Cascades, Channels, Weirs, and Spillways*. Oxford, U.K.: Pergamon.

Chanson, H. 2000. Characteristics of skimming flow over stepped spillways: Discussion. *J. Hydraul. Eng. ASCE* 125(4): 862-865.

Chanson, H. 2002. *The Hydraulics of Stepped Chutes and Spillways.* Steenwijk, The Netherlands: A. A. Balkema.

Chanson, H., and L. Toombes. 2002. Energy dissipation and air entrainment in a stepped storm waterway: An experimental study. *J. Irrig. and Drainage Eng. ASCE* 128(5): 305-315.

Chanson, H., Y. Yasuda, and I. Ohtsu. 2002. Flow resistance in skimming flows in stepped spillways and its modeling. *Canadian J. Civil Eng.* 29(6): 809-819.

Chatila, J. G., and B. R. Jurdi. 2004. Stepped spillway as an energy dissipater. *Canadian Water Resources J.* 29(3): 147-158.

Chow, V. T. 1959. *Open-Channel Hydraulics.* Boston, Mass.: McGraw-Hill.

Christodoulou, G. C. 1993. Energy dissipation on stepped spillways. *J. Hydraul. Eng. ASCE* 119(5): 644-655.

Felder, S., and H. Chanson. 2008. Turbulence and turbulent length and time scales in skimming flows on a stepped spillway: Dynamic similarity, physical modeling, and scale effects. Queensland, Australia: University of Queensland, Division of Civil Engineering.

Hunt, S. L., and K. C. Kadavy. 2007. Renwick dam RCC stepped spillway research. In *Proc. ASDSO Annual Meeting*, CD-ROM. Lexington, Ky.: Association of State Dam Safety Officials.

Hunt, S. L., and K. C. Kadavy. 2008. Energy dissipation on a 4(V):1(H) stepped spillway. In *Proc. ASDSO Annual Meeting*, CD-ROM. Lexington, Ky.: Association of State Dam Safety Officials.

Hunt, S. L., and K. C. Kadavy. 2009. Inception point relationship for flat-sloped stepped spillways. ASABE Paper No. 096571. St. Joseph, Mich.: ASABE.

Hunt, S. L., and K. C. Kadavy. 2010. Energy dissipation on flat-sloped stepped spillways: Part 1. Upstream of the inception point. *Trans. ASABE* 53(1): 103–109.

Hunt, S. L., K. C. Kadavy, S. R. Abt, and D. M. Temple. 2006. Converging RCC stepped spillways. In *Proc. 2006 World Environ. and Water Resources Congress, ASCE Conf.*, CD-ROM. Reston, Va.: ASCE.

Matos, J., K. H. Frizell, S. André, and K. W. Frizell. 2002. On performance of velocity measurement techniques in air-water flows. In *Proc. Hydraulic Measurements and Experimental Methods 2002*, CD-ROM. T. L. Wahl, C. A. Pugh, K. A. Oberg, and T. B. Vermeyen, eds. Reston, Va.: ASCE.

Peyras, L., P. Royet, and G. Degoutte. 1992. Flow and energy dissipation over stepped gabion weirs. *J. Hydraul. Eng. ASCE* 118(5): 707-717.

Rice, C. E., and K. C. Kadavy. 1996. Model study of a roller compacted concrete stepped spillway. *J. Hydraul. Eng. ASCE* 122(6): 92-297.

Takahashi, M., C. A. Gonzalez, and H. Chanson. 2006. Self-aeration and turbulence in a stepped channel: Influence of cavity surface roughness. *Intl. J. Multiphase Flow* 32(12): 1370-1385.

Yasuda, Y., and I. Ohtsu. 1999. Flow resistance of skimming flow in stepped channels. In *Proc. 28th IAHR Congress*, Session B14. International Association for Hydro-Environment Engineering and Research.